SUPPLEMENTARY INFORMATION

Insight into α-Synuclein Misfolding and Plasticity from Differential Micelle Binding

Parichita Mazumder, Jae-Eun Suk and Tobias S. Ulmer

Department of Biochemistry & Molecular Biology, Zilkha Neurogenetic Institute, Keck School of Medicine, University of Southern California, 1501 San Pablo Street, Los Angeles, CA 90033, USA

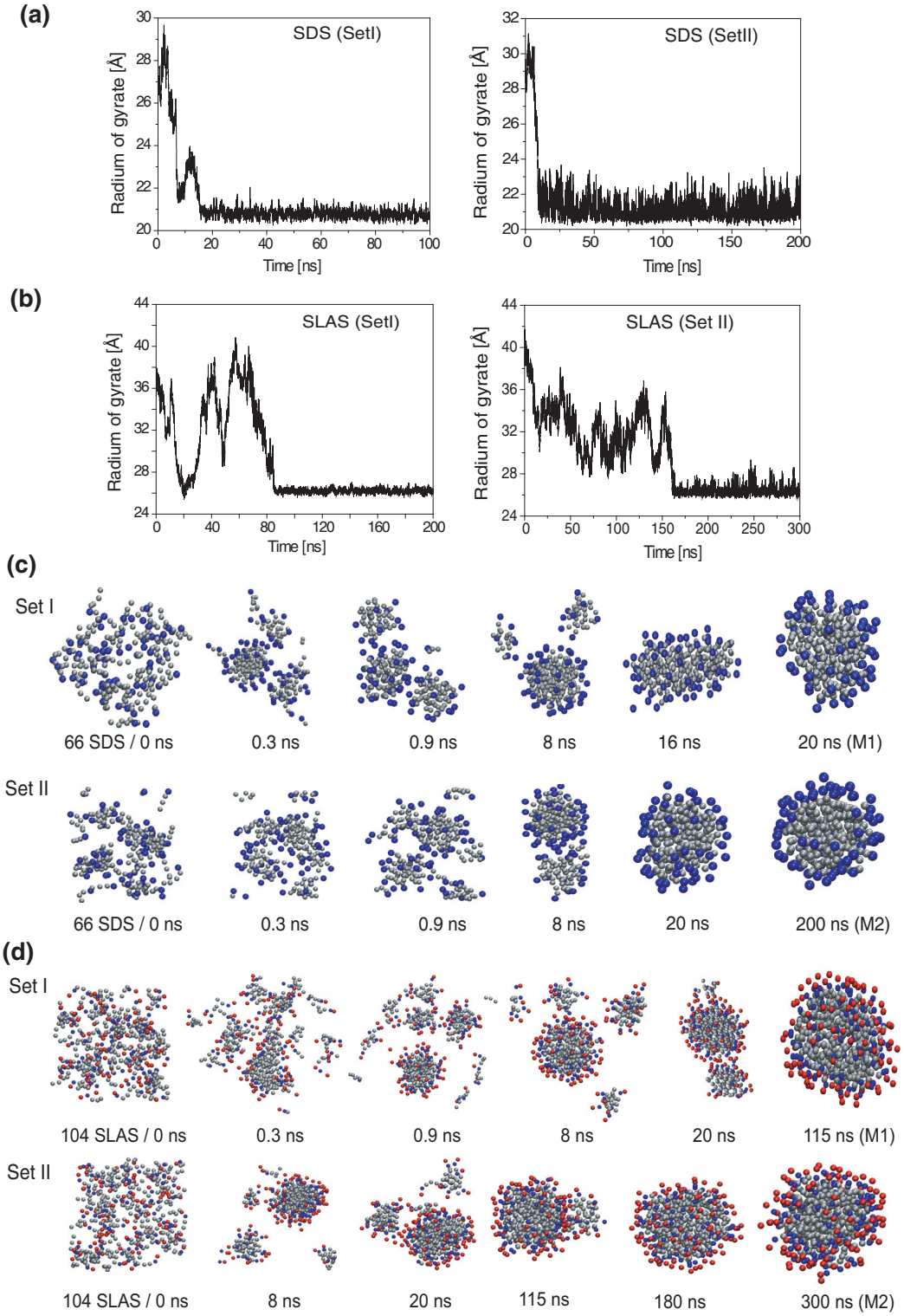

Figure S1. Coarse-grain (CG) molecular dynamics simulations of SDS and SLAS micelle assembly. (a-b) Average distance of head group beads from the center of micelle mass, radium of gyrate (R_g), as a function of simulation time. (c-d) Snapshots of detergent associations at the simulation times indicated. Simulations started from two random detergent molecule distributions (sets I and II). The resulting micelles are denoted M1 and M2, respectively. For visual clarity, water and sodium ions are not shown.

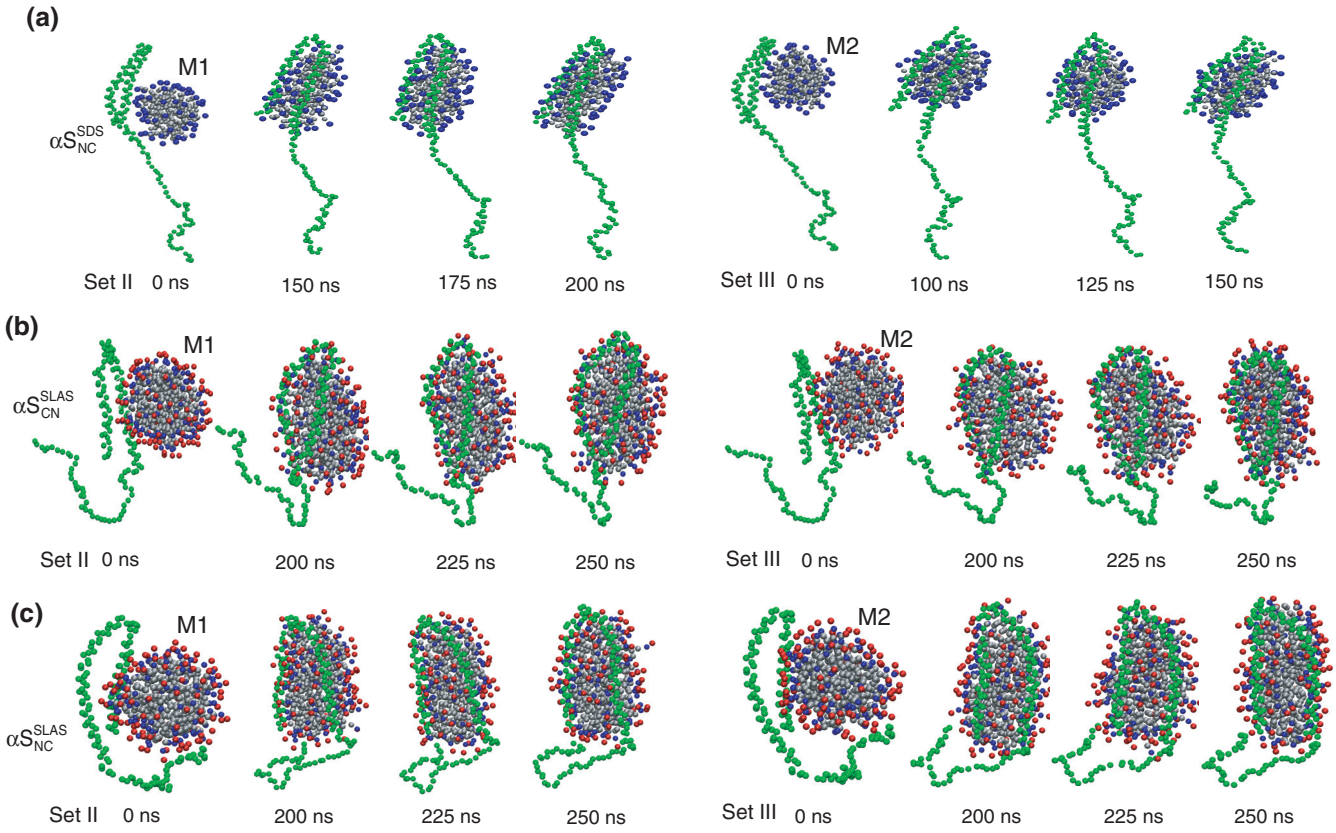

Figure S2. Micelle-αS complex formation during coarse-grained molecular dynamics simulations. (a-c) Complex formation of (a) αS^{SDS}_{NC}, (b) αS^{SLAS}_{CN} and (c) αS^{SLAS}_{NC} with pre-equilibrated micelles M1 and M2 (see Figure S1). A first set of association simulations is depicted in Figure 3d-f.

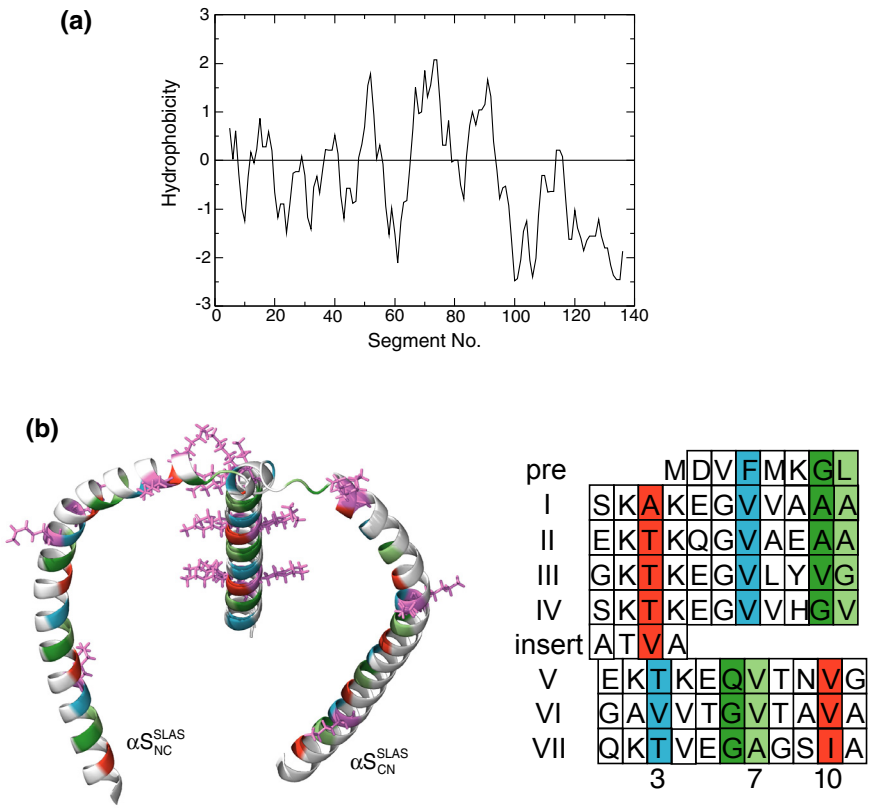

Figure S3. Sequence and spatial distribution of αS hydrophobicities. (a) Sequence distribution of αS hydrophobicity. The Kyte-Doolittle hydrophobicity scale was used with a window size of nine residues.[1] Center residues label segments. (b) Spatial distribution of membrane-facing residues for $\alpha S^{SLAS}{}_{NC}$ and $\alpha S^{SLAS}{}_{CN}$ structures. The residues that line the hydrophobic helix face are shown in color as depicted. The four-residue insert (Ala53-Ala56) changes the orientation of the membrane-facing helix faces with respect to its pseudorepeats sequence.[2]

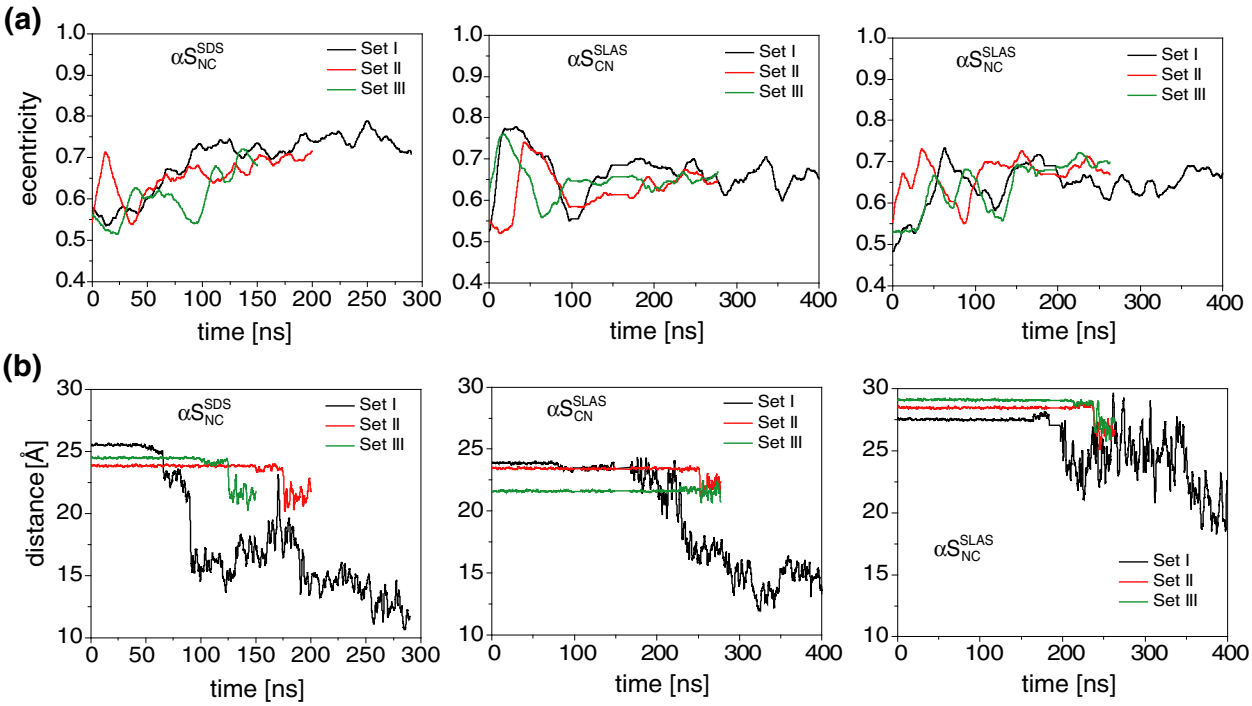

Figure S4. Evolution of structural parameter during CG MD simulations of micelle-bound αS. (a) Micelle eccentricity and (b) distance between backbone beads of αS residues A11 and V70 as a function of simulation time.

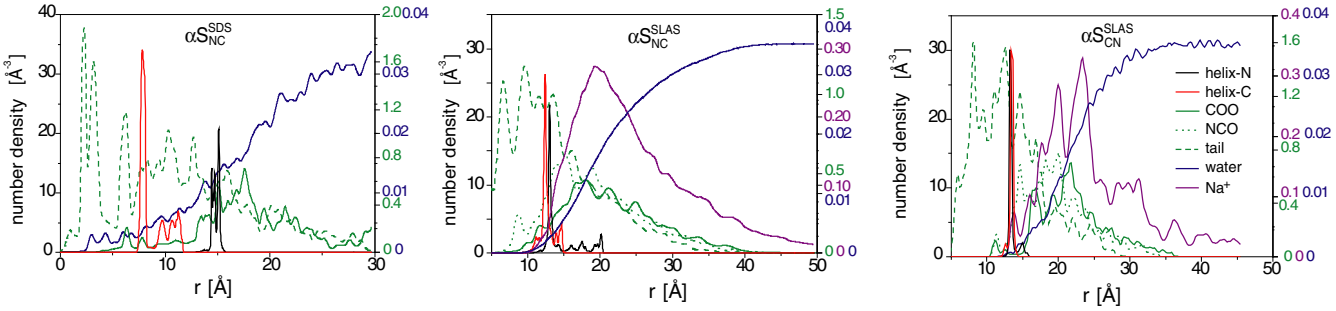

Figure S5. Association of partially folded αS with SDS and SLAS micelles in all atom MD simulations. Number density profiles of the indicated groups relative to the center of micelle mass. Profiles for all-atom MD simulations calculated for the time period of 50-100 ns. For SDS-αS^{SDS}_{NC}, the Na^+ distribution formed was ill-dispersed with no clear maxima and, for visual clarity, omitted.

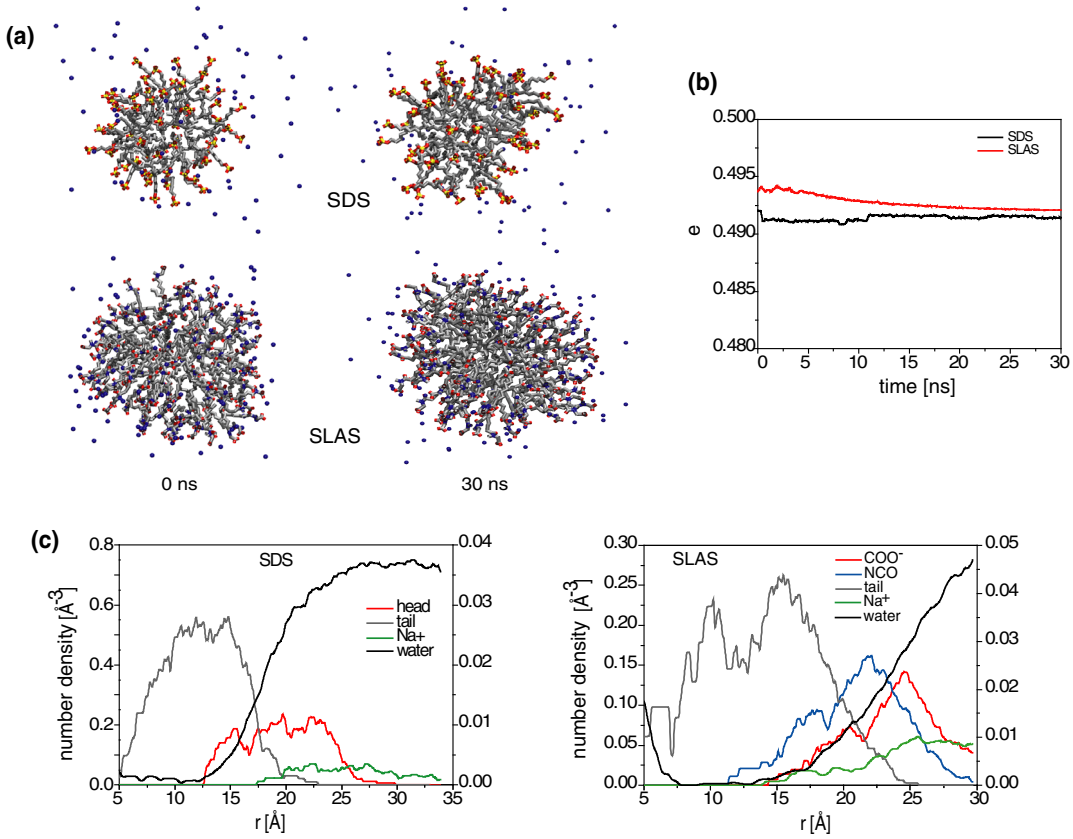

Figure S6. MD simulations of free SDS and SLAS micelles at atomic resolution. At the end of CG simulations (Figure S1a-b), CG configurations were transformed to atomistic coordinates using the reverse-transformation algorithm of GROMACS,[3] and all atom simulations were initiated. (a) Snapshots of detergent assemblies at the simulation times indicated. For clarity, water molecules were omitted. (b) Micelle eccentricity as a function of simulation time. (c) Number density profiles of the indicated groups relative to the micelle center of mass (COM) for the simulation period 5-30 ns.

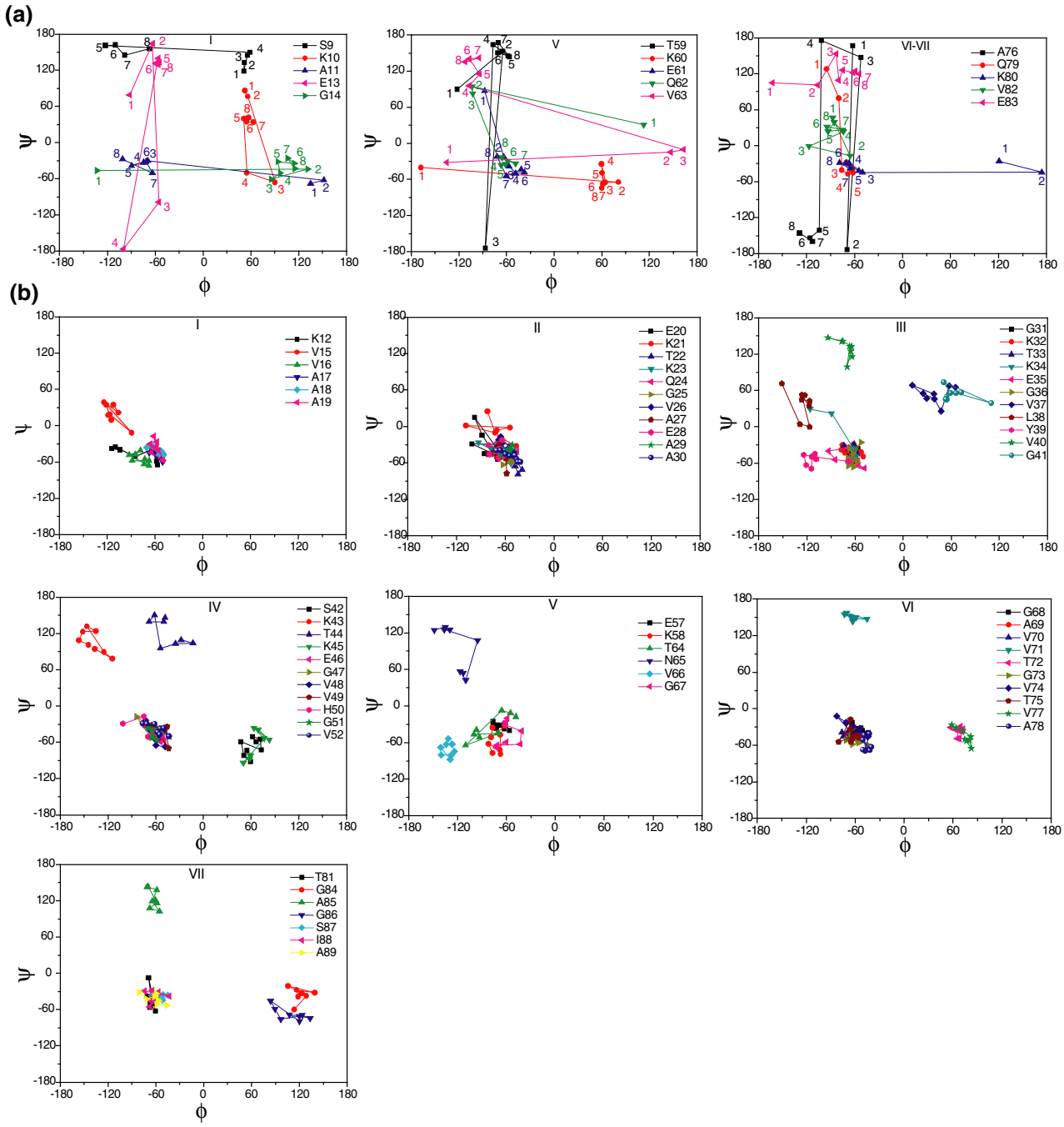

Figure S7. Evolution of backbone dihedral angles of αS^{SDS}_{NC} residues. (a) For relatively mobile residues, dihedral angles are shown at 0 ns (label 1), 20 ns (label 2), 40 ns (label 3), 50 ns (label 4), 60 ns (label 5), 70 ns (label 6), 80 ns (label 7) and 100 ns (label 8). (b) For less mobile residues, the same time points are shown without labels. In all panels, residues were grouped according to their αS pseudorepeat class (see Figure S3b).

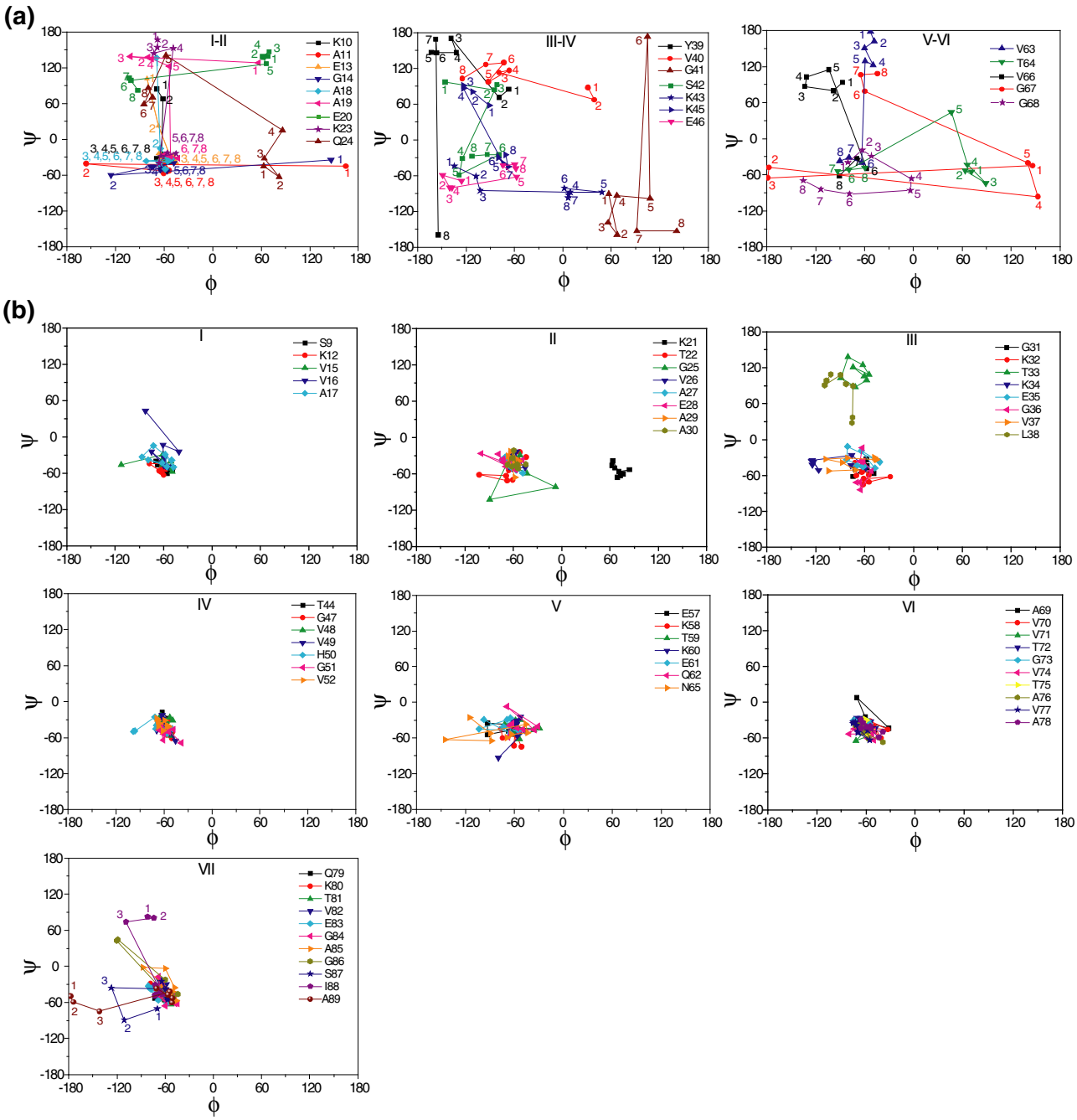

Figure S8. Evolution of backbone dihedral angles of αS^{SLAS}_{CN} residues. (a) For relatively mobile residues, dihedral angles are shown at 0 ns (label 1), 20 ns (label 2), 40 ns (label 3), 50 ns (label 4), 60 ns (label 5), 70 ns (label 6), 80 ns (label 7) and 100 ns (label 8). (b) For less mobile residues, the same time points are shown without labels. In all panels, residues were grouped according to their αS pseudorepeat class (see Figure S3b).

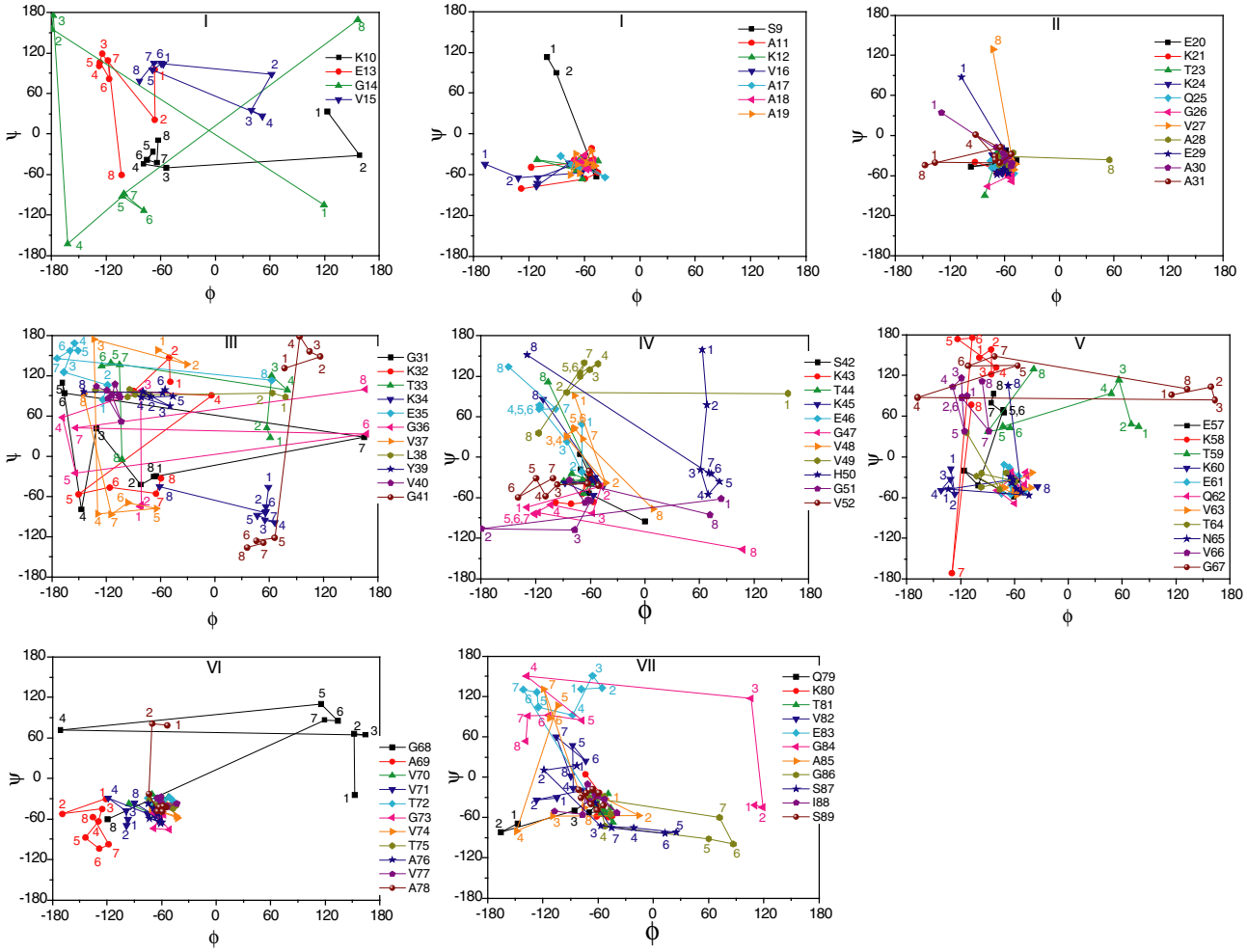

Figure S9. Evolution of backbone dihedral angles of αS^{SLAS}_{NC} residues. Dihedral angles are shown at 0 ns (label 1), 20 ns (label 2), 40 ns (label 3), 50 ns (label 4), 60 ns (label 5), 70 ns (label 6), 80 ns (label 7) and 100 ns (label 8). In all panels, residues were grouped according to their αS pseudorepeat class (see Figure S3b).

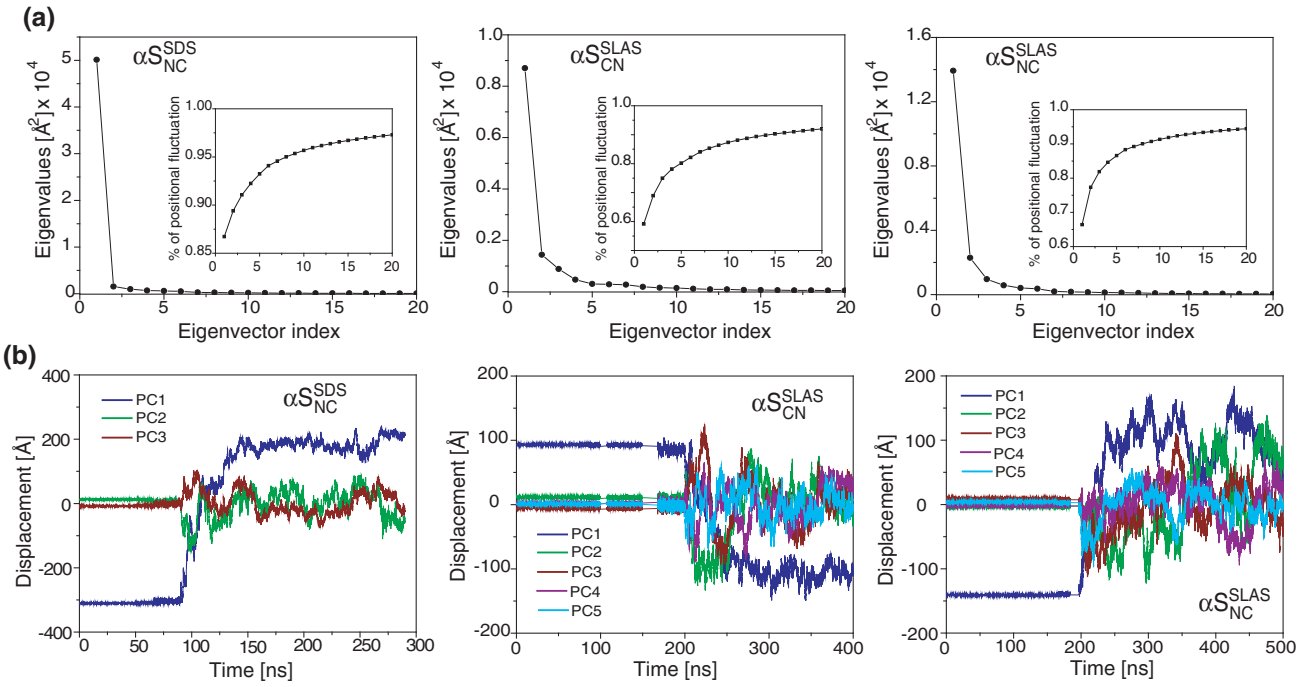

Figure S10. Principal component analysis (PCA) of αS-micelle complex CG-MD simulations. (a) The 20 largest eigenvalues obtained for the simulations of Figure 3d-f shown in descending order. The inserts depict the percentage of fluctuations captured by the corresponding eigenvectors. (b) Fluctuations along the directions of the indicated eigenvector or principal components (PC) as a function of simulation time.

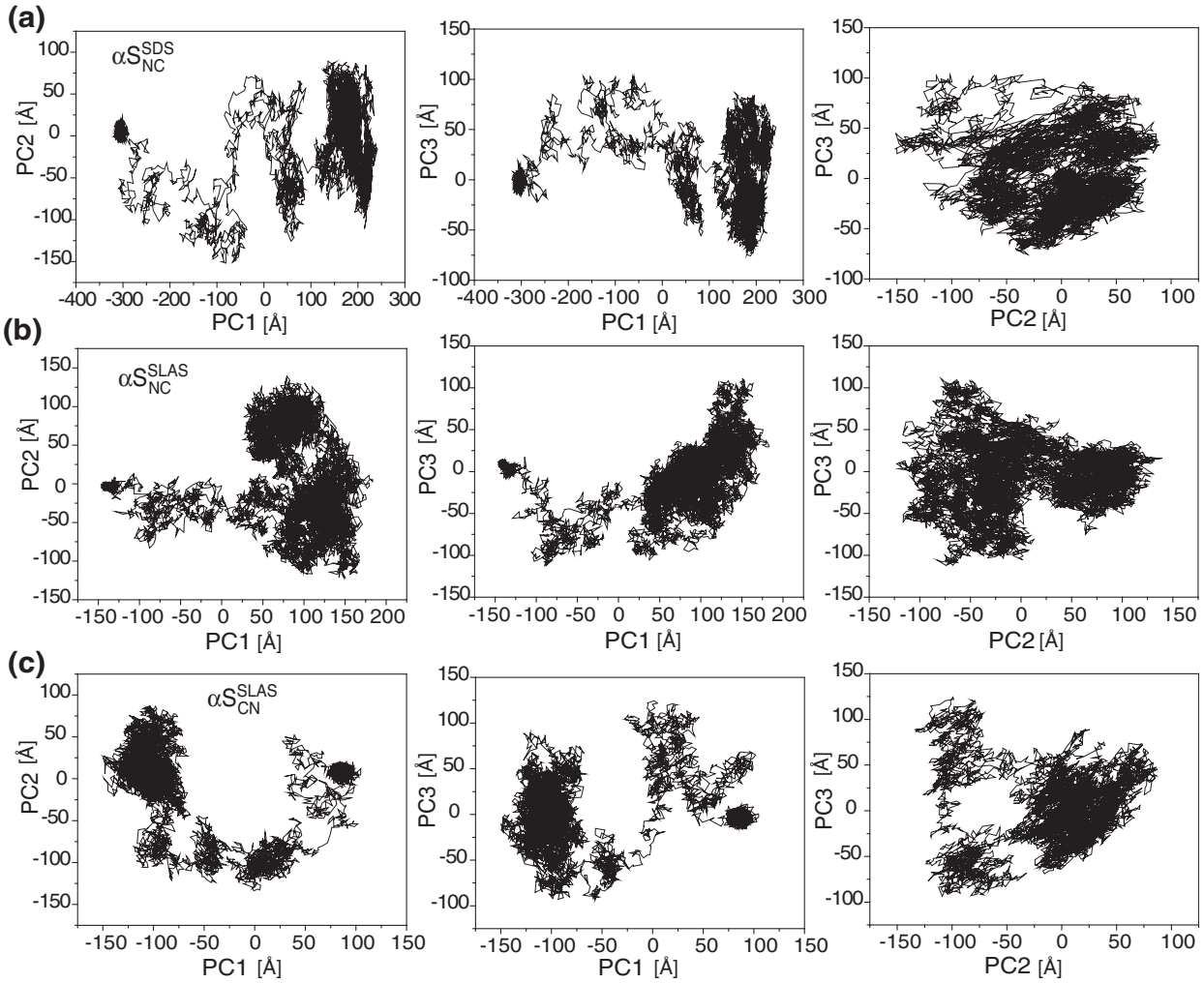

Figure S11. Projections of the (a) αS^{SDS}_{NC}, (b) αS^{SLAS}_{NC} and (c) αS^{SLAS}_{CN} CG MD trajectories on planes defined by two principal components (eigenvectors) as indicated.

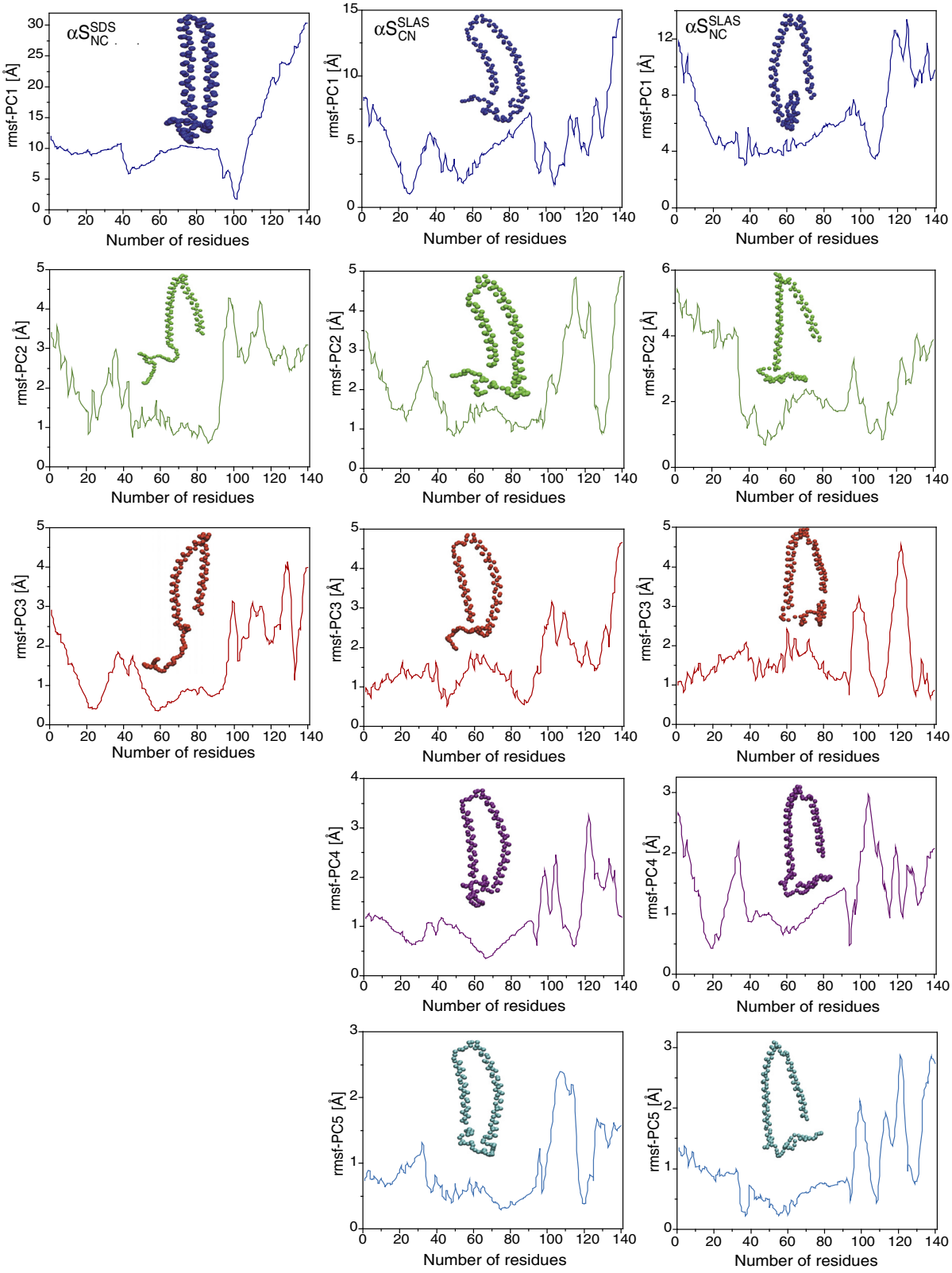

Figure S13. Root-mean-square fluctuations (RMSF) of amino acid beads projected along the depicted principal components (PC) as a function of αS residue number.

Table S1. Micelle parameter of SLAS and SDS.[a]

Detergent	Radius [Å]	Mass [kDa]	Aggregation number
SLAS[b]	22.2	30.6	104
SDS	18.7	19.0	66

[a]In 25 mM NaH_2PO_4/Na_2HPO_4, pH 7.4, solution.
[b]Values taken from Rao et al.[2]

Table S2. Coarse-grain topology for SLAS.

SLAS_cg.itp

```
[ moleculetype ]
; molname       nrexcl
  SLA           1

[atoms]
; id    type    resnr   residu  atom     cgnr    charge
  1     Qa      1       SLA     COO        1       -1.0
  2     Na      1       SLA     NCO        2       0
  3     C2      1       SLA     C1         3       0
  4     C1      1       SLA     C2         4       0
  5     C1      1       SLA     C3         5       0

[bonds]
; i j   funct   length  force.c.
  1 2   1       0.47    1250
  2 3   1       0.47    1250
  3 4   1       0.47    1250
  4 5   1       0.47    1250

[angles]
; i j k         funct   angle   force.c.
  2 3 4         2       180.0   25.0
  3 4 5         2       180.0   25.0
```

SLAS_CG.pdb

```
ATOM    1  COO SLA   1      42.725  52.470  68.035  1.00  0.00
ATOM    2  NCO SLA   1      43.187  52.533  63.096  1.00  0.00
ATOM    3  C1  SLA   1      44.103  51.565  59.097  1.00  0.00
ATOM    4  C2  SLA   1      43.251  48.483  55.518  1.00  0.00
ATOM    5  C3  SLA   1      45.554  46.307  51.858  1.00  0.00
TER
END
```

Table S3. Summary of repeated coarse-grained (CG) simulations.

Simulation	No. of water beads / atoms	Total no. of beads / atoms	Box dimension [Å]	Simulation time [ns]
CG (micelle self-assembly)[a,c]				
SDS (M1)	2,383	2,713	68×68×68	100
(M2)	2,391	2,721	65×65×65	200
SLAS (M1)	8,630	9,254	100×100×100	200
(M2)	6,086	6,710	80×80×80	300
CG (micelle pre-equilibrated)[b,c]				
SDS-αS^{SDS}_{NC} (set I)	6,739	7,350	60×240 ×60	300
(set II)	10,295	10,906	70×240×70	200
(set III)	13,210	13,821	80×240×70	150
SLAS-αS^{SLAS}_{CN} (set I)	8,051	8,956	61×88×95	400
(set II)	18,318	19,223	100×120×160	250
(set III)	19,935	20,840	100×140×160	250
SLAS-αS^{SLAS}_{NC} (set I)	10,008	10,913	120×100×100	400
(set II)	10,367	11,272	120×90×100	250
(set III)	12,271	13,176	120×90×110	250

[a] M1 and M2 denotes the two micelle simulations of Figure S1.
[b] Three sets of αS-micelle CG simulations were performed (Figure 3d-f and Figure S2).
[c] 264 SDS, 520 SLAS and 272 αS beads were employed.

Table S4. Fine-grain topology for SLAS.

SLAS_fg.itp

```
[ moleculetype ]
; Name nrexcl
SLA      3

[ atoms ]
;   nr       type  resnr resid  atom  cgnr   charge     mass
     1         O      1  SLA     O       1   -0.465  15.9994
     2         C      1  SLA     C1      1    0.380  12.0110
     3        OM      1  SLA     OM      1   -0.635  15.9994
     4       CH2      1  SLA     C2      1    0.000  14.0270
     5         N      1  SLA     N       1   -0.280  14.0067
     6       CH3      1  SLA     C3      2    0.000  15.0350
     7         C      1  SLA     C4      2    0.380  12.0110
     8         O      1  SLA     O       2   -0.380  15.9994
     9       CH2      1  SLA     C5      2    0.000  14.0270
    10       CH2      1  SLA     C6      2    0.000  14.0270
    11       CH2      1  SLA     C7      2    0.000  14.0270
    12       CH2      1  SLA     C8      2    0.000  14.0270
    13       CH2      1  SLA     C9      3    0.000  14.0270
    14       CH2      1  SLA     C10     3    0.000  14.0270
    15       CH2      1  SLA     C11     3    0.000  14.0270
    16       CH2      1  SLA     C12     3    0.000  14.0270
    17       CH2      1  SLA     C13     3    0.000  14.0270
    18       CH2      1  SLA     C14     3    0.000  14.0270
    19       CH3      1  SLA     C15     3    0.000  15.0350

[ bonds ]
; ai  aj  fu    c0, c1, ...
   2   1   2    0.125  13400000.0
   2   3   2    0.125  13400000.0
   2   4   2    0.153   7150000.0
   5   4   2    0.147   8710000.0
   5   6   2    0.147   8710000.0
   5   7   2    0.134  10500000.0
   7   8   2    0.136  10200000.0
   7   9   2    0.153   7150000.0
   9  10   2    0.153   7150000.0
  10  11   2    0.153   7150000.0
  11  12   2    0.153   7150000.0
  12  13   2    0.153   7150000.0
  13  14   2    0.153   7150000.0
  14  15   2    0.153   7150000.0
  15  16   2    0.153   7150000.0
  16  17   2    0.153   7150000.0
  17  18   2    0.153   7150000.0
  18  19   2    0.153   7150000.0

[ pairs ]
; ai  aj  fu    c0, c1, ...
   1   5   1
   2   6   1
   2   7   1
   3   5   1
   4   8   1
   4   9   1
   5  10   1
   6   8   1
```

```
   6   9   1
   7  11   1
   8  10   1
   9  12   1
  10  13   1
  11  14   1
  12  15   1
  13  16   1
  14  17   1
  15  18   1
  16  19   1

[ angles ]
; ai  aj  ak  fu    c0, c1, ...
   1   2   3   2    126.0       770.0
   1   2   4   2    117.0       635.0
   3   2   4   2    117.0       635.0
   2   4   5   2    109.5       520.0
   4   5   6   2    121.0       685.0
   4   5   7   2    122.0       700.0
   6   5   7   2    117.0       635.0
   5   7   8   2    124.0       730.0
   5   7   9   2    115.0       610.0
   8   7   9   2    115.0       610.0
   7   9  10   2    109.5       520.0
   9  10  11   2    109.5       520.0
  10  11  12   2    109.5       520.0
  11  12  13   2    109.5       520.0
  12  13  14   2    109.5       520.0
  13  14  15   2    109.5       520.0
  14  15  16   2    109.5       520.0
  15  16  17   2    109.5       520.0
  16  17  18   2    109.5       520.0
  17  18  19   2    109.5       520.0

[ dihedrals ]
; ai  aj  ak  al  fu    c0, c1, m, ...
   2   1   3   4   2      0.0  167.4
   5   4   6   7   2      0.0  167.4
   7   5   8   9   2      0.0  167.4
   5   4   2   1   1      0.0    1.06
   2   4   5   7   1    180.0    1.06
   9   7   5   4   1    180.0   33.52
  10  11   7   5   1      0.0    1.06
  11  12   9   7   1      0.0    5.93
  12  11  10   9   1      0.0    5.93
  13  12  11  10   1      0.0    5.93
  14  13  12  11   1      0.0    5.93
  15  14  13  12   1      0.0    5.93
  16  15  14  13   1      0.0    5.93
  17  16  15  14   1      0.0    5.93
  18  17  16  15   1      0.0    5.93
  19  18  17  16   1      0.0    5.93
```

Supplemental References

(1) Kyte, J.; Doolittle, R. F. A Simple Method for Displaying the Hydropathic Character of a Protein. *J. Mol. Biol.* **1982**, *157*, 105.
(2) Rao, J. N.; Kim, Y. E.; Park, L. S.; Ulmer, T. S. Effect of Pseudorepeat Rearrangement on Alpha-Synuclein Misfolding, Vesicle Binding, and Micelle Binding. *J. Mol. Biol.* **2009**, *390*, 516-529.
(3) Rzepiela, A. J.; Schafer, L. V.; Goga, N.; Risselada, H. J.; De Vries, A. H.; Marrink, S. J. Software News and Update Reconstruction of Atomistic Details from Coarse-Grained Structures. *J. Comput. Chem.* **2010**, *31*, 1333-1343.